NK cells promote transplant tolerance by killing donor antigen-presenting cells

Guang Yu, Xuemin Xu, Minh Diem Vu, Elizabeth D. Kilpatrick, and Xian Chang Li

Transplant Research Center, Department of Medicine and Department of Surgery, Beth Israel Deaconess Medical Center, Harvard Medical School, Boston MA 02215

Natural killer (NK) cells are programmed to kill target cells without prior antigen priming. Because of their potent cytolytic activities, NK cells are one of the key cell types involved in dismantling allografts. However, in certain transplant models, NK cells also express potent immunoregulatory properties that promote tolerance induction. The precise mechanism for such striking dichotomy remains unknown. In the present study, we showed in a skin transplant model that the skin allografts contain a subset of antigen-presenting cells (APCs) that can home to the recipient mice. We also showed that such graft-derived APCs are usually destroyed by the host NK cells. But in the absence of NK cells, donor APCs can survive and then migrate to the host lymphoid and extralymphoid sites where they directly stimulate the activation of alloreactive T cells. T cells activated in the absence of NK cells are more resistant to costimulatory blockade treatment, and under such conditions stable skin allograft survival is difficult to achieve. Our study identified a novel role for NK cells in regulating T cell priming in transplant models, and may have important clinical implications in tolerance induction.

CORRESPONDENCE
Xian C. Li:
xli@bidmc.harvard.edu

NK cells are a major cell type in the innate immune system (1). Unlike T cells in the adaptive system, the innate NK cells are programmed to kill targets without prior antigen priming (1). The cytolytic activity of NK cells is tightly controlled by a group of cell surface receptors that can deliver either stimulatory or inhibitory signals, and engagement of inhibitory receptors by the self-MHC class I molecules is a principal mechanism by which NK-mediated damage to self is prevented (2, 3). However, NK cells are highly cytotoxic to target cells mismatched for the MHC class I molecules (4, 5) or autologous cells with down-regulated expression of self-MHC class I molecules (missing self theory) (3, 5). Thus, NK cells often function as potent effector cells in rejection of allogeneic bone marrow cells (6) and solid organ transplants (7, 8). In certain models, however, NK cells also express potent immunoregulatory properties that promote transplant tolerance (9), but the mechanisms are poorly defined. A key question that remains to be answered is how the innate cells would regulate the adaptive T cell response in transplant models, especially in tolerance induction.

Unlike any other models, priming of T cells for the rejection response in transplant models is induced primarily by the graft-derived donor APCs (i.e., direct antigen presentation), albeit host APCs with processed allogeneic peptides (indirect pathway) also contribute to the rejection response (10). This is because of the presence of large numbers of donor APCs normally residing in transplanted organs. It is well known that priming by the direct pathway often activates an unusually large mass of alloreactive T cell clones, which constitutes one of the potent barriers to the induction of transplant tolerance (11). As the presence of host secondary lymphoid organs (e.g., spleen and lymph nodes) is mandatory for direct T cell priming and acute allograft rejection (12, 13), we hypothesized that survival and dissemination of graft-derived donor APCs in transplant recipients may critically affect the nature of the rejection response and the susceptibility to tolerance induction. In the present study, we found that host NK cells play a critical role in regulating the life and death of donor-derived APCs, thereby affecting the locations and pathways of T cell priming in transplant tolerance induction.

The Journal of Experimental Medicine

RESULTS AND DISCUSSION

To definitively determine the role of NK cells in transplant models, we transplanted the DBA/2 skin allografts (H-2^d) onto the Rag deficient (Rag$^{-/-}$) and Rag plus the common γc double-deficient mice (Rag$^{-/-}$γc$^{-/-}$) (H-2^b), and examined the skin allograft survival and the fate of graft-derived APCs in the recipient mice. Both Rag$^{-/-}$ and Rag$^{-/-}$γc$^{-/-}$ mice are deficient for T cells and B cells. Unlike the

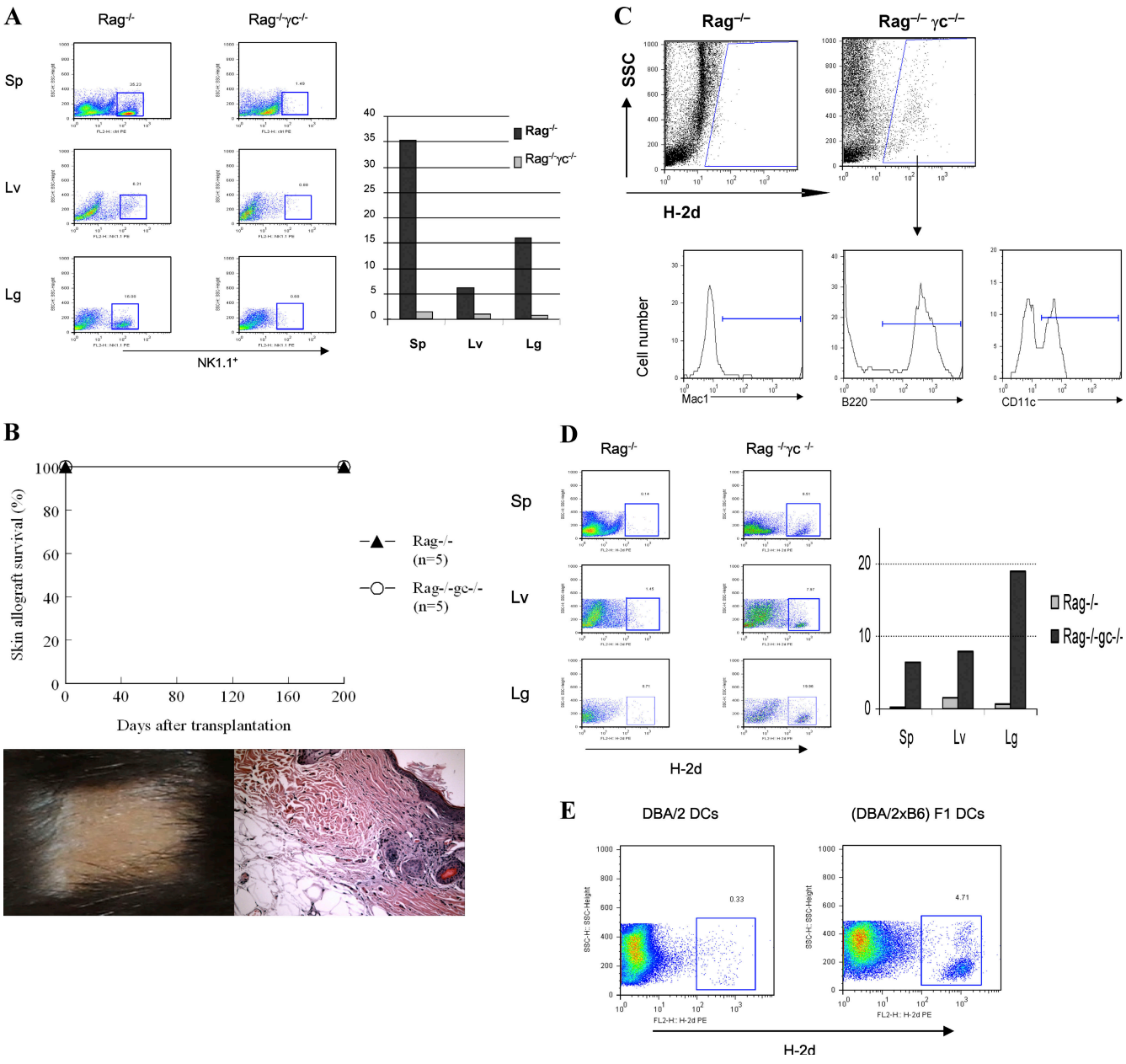

Figure 1. NK cells in survival of skin allograft and graft-derived APCs. (A) Staining for NK cells in Rag$^{-/-}$ and Rag$^{-/-}$γc$^{-/-}$ mice. Cells were prepared from the spleen (Sp), liver (Lv), and lungs (Lg) of Rag$^{-/-}$ and Rag$^{-/-}$γc$^{-/-}$ mice and examined for the presence of NK1.1$^+$ cells. Data from four individual experiments are shown. (B) Long-term survival of DBA/2 skin allografts transplanted onto Rag$^{-/-}$ and Rag$^{-/-}$γc$^{-/-}$ mice. Pictures shown are representative of skin allografts and tissue histology at 200 d after transplantation. (C) Analysis of graft-derived donor cells in Rag$^{-/-}$ and Rag$^{-/-}$γc$^{-/-}$ mice transplanted with DBA/2 skin allografts. Spleen cells were prepared from the Rag$^{-/-}$ and Rag$^{-/-}$γc$^{-/-}$ mice 30 d after grafting with DBA/2 skin allografts. The spleen cells were then stained with PE anti-H-2D^d mAb to determine the presence or absence of donor-derived cells. Representative data of three individual experiments are shown. (D) Survival and dissemination of allogeneic donor DCs in Rag$^{-/-}$ and Rag$^{-/-}$γc$^{-/-}$ hosts. MACS sorted CD11c$^+$ DCs from DBA/2 donors were injected into Rag$^{-/-}$ and Rag$^{-/-}$γc$^{-/-}$ recipients. 2 wk later, the host mice were killed and cells were prepared from the spleen (Sp), liver (Lv), and lungs (Lg), followed by staining with PE anti-H-2D^d mAb to determine donor-origin cells. Representative plot of four individual experiments is shown. (E) Survival of (DBA/2 x B6)F1 DCs but not DBA/2 DCs in Rag$^{-/-}$ hosts.

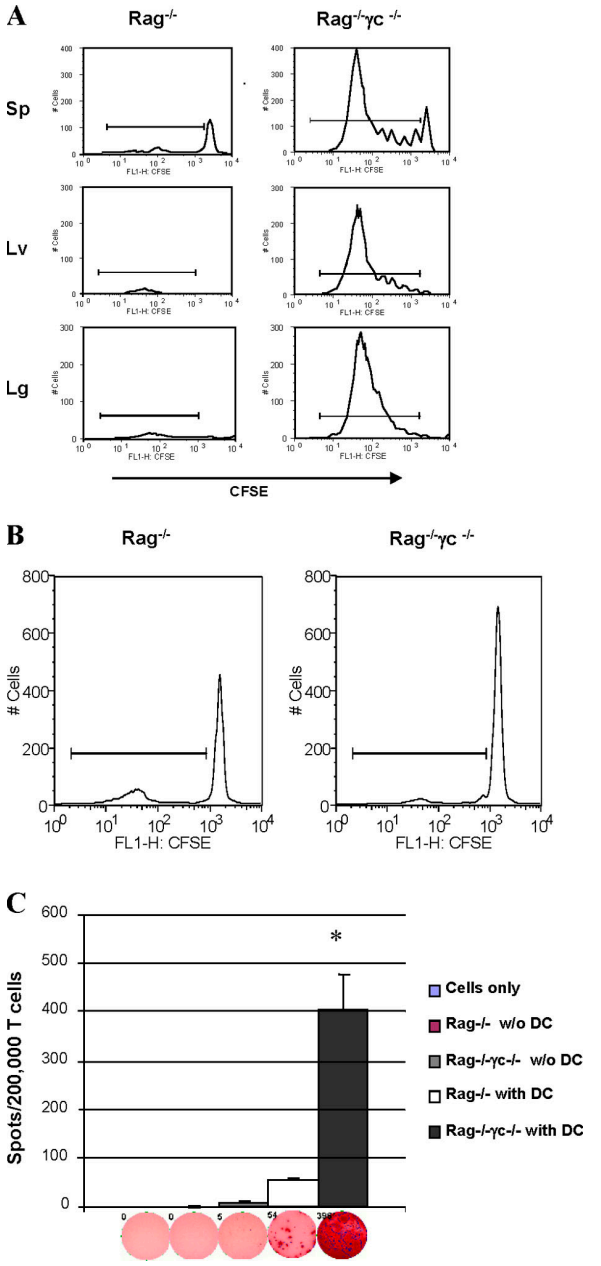

Figure 2. T cell activation in vivo with or without NK cells. (A) Proliferation of T cells adoptively transferred into $Rag^{-/-}$ and $Rag^{-/-}\gamma c^{-/-}$ mice injected with allogeneic DBA/2 DCs. $CD11c^+$ DCs prepared from DBA/2 donors were injected into $Rag^{-/-}$ and $Rag^{-/-}\gamma c^{-/-}$ recipients ($\sim 6 \times 10^6$ DCs per mouse). 2 wk later, each mouse was reconstituted with $\sim 20 \times 10^6$ CFSE-labeled syngeneic C57BL/6 T cells. Proliferation of T cells in the host spleen, liver, and lungs was determined 3 d later by gating onto the $CD3^+$ fraction. Similar data were obtained in four independent experiments. (B) Proliferation of T cells adoptively transferred into $Rag^{-/-}$ and $Rag^{-/-}\gamma c^{-/-}$ mice without injection of allogeneic DCs. CFSE-labeled syngeneic T cells were transferred into $Rag^{-/-}$ and $Rag^{-/-}\gamma c^{-/-}$ mice (20×10^6 cells per mouse) and analyzed 3 d later by gating onto the $CD3^+$ fraction. Similar data were obtained in three individual experiments. (C) Production of IFN-γ by T cells transferred into $Rag^{-/-}$ and $Rag^{-/-}\gamma c^{-/-}$ mice injected with allogeneic DBA/2 DCs. $CD11c^+$ DCs from DBA/2 donors were injected into $Rag^{-/-}$ and $Rag^{-/-}\gamma c^{-/-}$ mouse. 2 wk later, each mouse was reconstituted with $\sim 20 \times 10^6$ CFSE-labeled syngeneic C57BL/6 T cells. T cells were isolated from the host spleen 3 d later and restimulated ex vivo with donor DBA/2 cells for 24 h, and production of IFN-γ was determined by ELISPOT. Data are presented as mean ± SD spots of triplicate assays. *$P < 0.05$.

$Rag^{-/-}\gamma c^{-/-}$ mice, which are also deficient for NK cells (14), the $Rag^{-/-}$ mice have a large population of NK cells in the periphery (Fig. 1 A). Thus, the effects of NK cells against the DBA/2 skin allografts and their residing donor APCs can be directly studied.

Both $Rag^{-/-}$ and $Rag^{-/-}\gamma c^{-/-}$ mice permanently accepted the DBA/2 skin allografts (>200 d, $n = 5$) without any gross or histological signs of rejection (Fig. 1 B). However, the fate of graft-derived donor APCs in the $Rag^{-/-}$ and $Rag^{-/-}\gamma c^{-/-}$ hosts was strikingly different. In the $Rag^{-/-}\gamma c^{-/-}$ mice, donor APCs could be readily identified in the host spleen. Such graft-derived cells included $CD11c^+$ DCs (Fig. 1 C), a cell type that undoubtedly contributes to the high immunogenicity of the skin grafts (15). In contrast, such donor APCs were completely absent in the $Rag^{-/-}$ hosts. This striking difference concerning the presence or absence of donor APCs in $Rag^{-/-}$ and $Rag^{-/-}\gamma c^{-/-}$ mice persisted for a long period of time after skin transplantation (30–100 d later). This finding suggests that NK cells may play a particularly important role in regulating the survival and dissemination of donor APCs in transplant recipients.

To further address this issue, we purified $CD11c^+$ DCs from DBA/2 donors and adoptively transferred them into $Rag^{-/-}$ and $Rag^{-/-}\gamma c^{-/-}$ mice ($\sim 6 \times 10^6$ DCs/mouse). Survival and dissemination of the allogeneic DCs in the host mice was determined 2 wk later. As shown in Fig. 1 D, DBA/2 DCs were completely destroyed upon transferring into the $Rag^{-/-}$ mice, and such cells could no longer be found in either the spleen or the extralymphoid tissues (i.e., liver and lungs). In sharp contrast, the allogeneic DBA/2 DCs could be readily recovered from the spleen of $Rag^{-/-}\gamma c^{-/-}$ mice. Importantly, such allogeneic DCs also accumulated in large numbers in the extralymphoid organs in $Rag^{-/-}\gamma c^{-/-}$ hosts (Fig. 1 D). Destruction of allogeneic DCs is mediated primarily by host NK cells as DCs from (DBA/2 x B6) F1 mice survived well in the $Rag^{-/-}$ mice (Fig. 1 E). Hence, the presence or absence of NK cells can have a profound impact on life and death of fully MHC mismatched donor APCs in vivo.

To determine whether the donor DCs homing to the host mice could stimulate the activation of alloreactive T cells, we again purified DCs from DBA/2 mice and transferred them into $Rag^{-/-}$ and $Rag^{-/-}\gamma c^{-/-}$ mice. 2 wk later, the host mice were reconstituted with CFSE-labeled syngeneic C57BL/6 T cells ($\sim 20 \times 10^6$/mouse). Proliferation of syngeneic T cells in different compartments of the host mice was examined 3 d later. As shown in Fig. 2 A, the adoptively transferred T cells readily accumulated in both

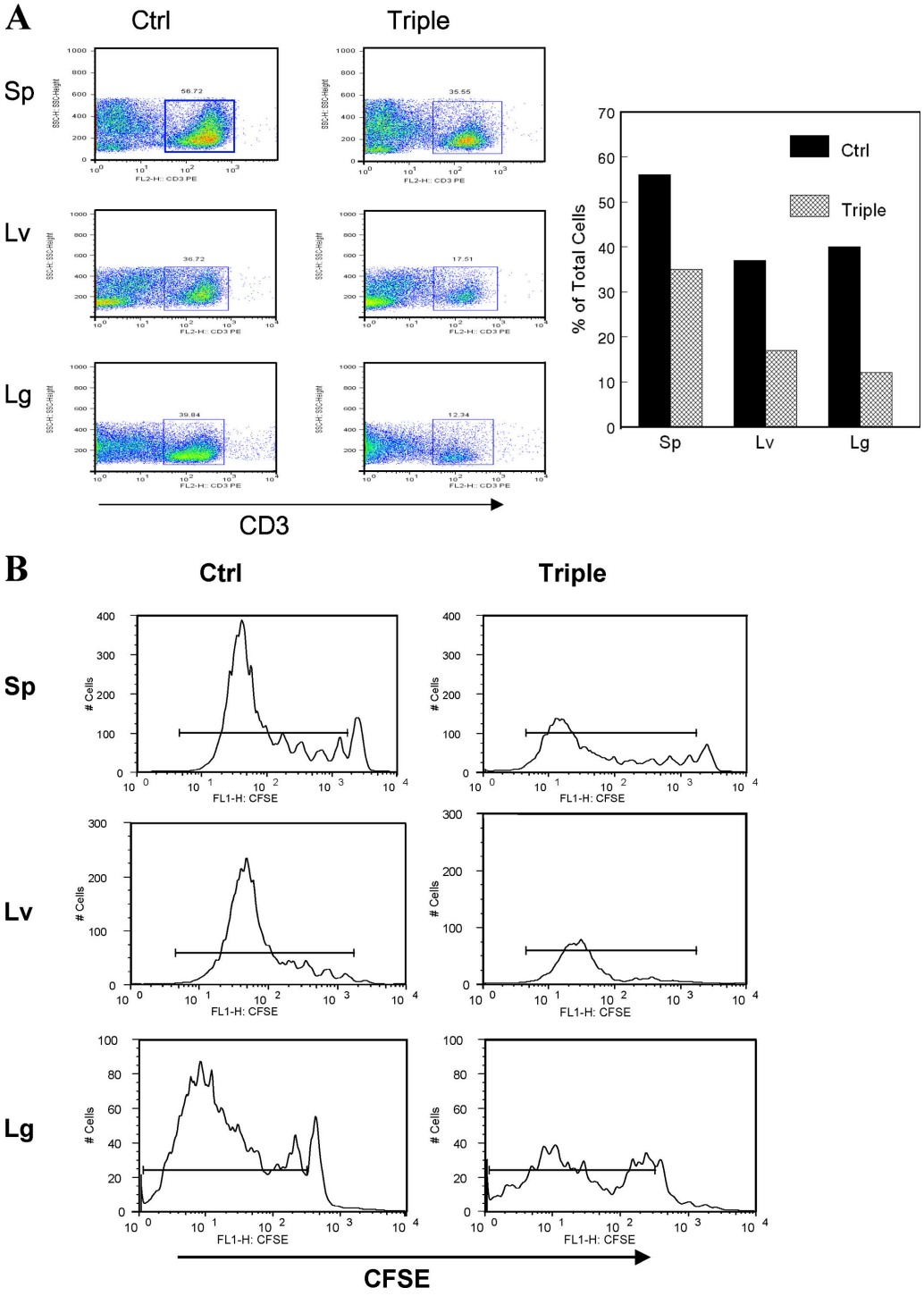

Figure 3. Effect of costimulatory blockade on T cell activation in vivo in the absence of NK cells. (A) Recovery of transferred T cells from $Rag^{-/-}\gamma c^{-/-}$ mice injected with allogeneic DBA/2 DCs and treated with CD28/CD154/OX40 costimulatory blockade. $CD11c^{+}$ DCs from DBA/2 donors were injected into $Rag^{-/-}\gamma c^{-/-}$ hosts. 2 wk later, each mouse was reconstituted with ~20 × 10^6 CFSE-labeled syngeneic C57BL/6 T cells. Some $Rag^{-/-}\gamma c^{-/-}$ hosts were also treated with CD28/CD154/OX40 blockade protocol. Recovery of $CD3^{+}$ T cells in the host spleen, liver, and lungs was determined 3 d later. Representative data of three individual experiments are shown. (B) Effect of blocking CD28/CD154/OX40 costimulation on proliferation of adoptively transferred T cells in $Rag^{-/-}\gamma c^{-/-}$ mice injected with allogeneic DBA/2 DCs. The $Rag^{-/-}\gamma c^{-/-}$ mice were prepared as described in Fig. 3 A, and proliferation of T cells at different sites of $Rag^{-/-}\gamma c^{-/-}$ mice was determined 3 d later by gating onto the $CD3^{+}$ fraction. Representative data of three individual experiments are shown.

the spleen and the extralymphoid organs in $Rag^{-/-}\gamma c^{-/-}$ hosts. In the $Rag^{-/-}$ mice, however, such T cells primarily accumulated in the spleen but not in the extralymphoid organs. Analysis of their CFSE profile revealed that most of the T cells recovered from the $Rag^{-/-}$ mice did not enter the cell cycle and, therefore, remained undivided (Fig. 2 A). In contrast, T cells from the $Rag^{-/-}\gamma c^{-/-}$ mice divided vigorously, and multiple rounds of cell divisions could be clearly identified. Such vigorous T cell division in $Rag^{-/-}\gamma c^{-/-}$ mice was observed not only in the spleen but also in the extralymphoid sites. Adoptive transfer of syngeneic T cells only ($\sim 20 \times 10^6$/mouse) into $Rag^{-/-}$ and $Rag^{-/-}\gamma c^{-/-}$ mice without donor DCs did not induce marked T cell proliferation in vivo (Fig. 2 B). Thus, the large number of T cells injected ($\sim 20 \times 10^6$/mouse) and the time point examined (only 3 d) did not induce homeostatic proliferation (16); and T cell proliferation in this model is induced primarily by donor DCs.

To further examine the effector functions of T cells transferred into $Rag^{-/-}$ and $Rag^{-/-}\gamma c^{-/-}$ mice with or without prior injection of allogeneic DCs, T cells were recovered from the host mice 3 d later and restimulated ex vivo with donor antigens and production of IFN-γ was assessed by ELISPOT assay. As shown in Fig. 2 C, T cells recovered from $Rag^{-/-}$ and $Rag^{-/-}\gamma c^{-/-}$ mice without prior injection of donor DCs did not produce detectable levels of IFN-γ. In contrast, T cells recovered from $Rag^{-/-}\gamma c^{-/-}$ mice injected with donor DCs readily produced a copious amount of IFN-γ ($\sim$400 spots/200,000 T cells), which was $\sim$8 times higher than those from $Rag^{-/-}$ mice ($\sim$50 spots/200,000 T cells). Similar findings were observed for T cells recovered from the liver and the lungs (unpublished data). These findings strongly suggest that, in the absence of NK cells, the injected allogeneic DCs survived and then migrated to the host spleen and extralymphoid sites where they directly stimulated the activation and effector function of alloreactive T cells.

Clearly, NK cells have a profound impact on life and death of donor APCs in transplant recipients. To determine the activation requirement of T cells stimulated by the donor DCs in the host mice, we reconstituted the $Rag^{-/-}\gamma c^{-/-}$ mice with CFSE-labeled syngeneic T cells 2 wk after injection of allogeneic DBA/2 DCs. The host mice were then treated with CTLA-4Ig, anti-CD154, and anti-OX40L to transiently block CD28/CD154/OX40 costimulatory pathways (triple costimulatory blockade), and proliferation of T cells in the $Rag^{-/-}\gamma c^{-/-}$ mice was examined 3 d later. As shown in Fig. 3 A, treatment of host mice with CD28/CD154/OX40 costimulatory blockade protocol resulted in a marked reduction of T cell recovery compared with untreated controls, suggesting that blocking CD28/CD154/OX40 costimulatory pathways may inhibit T cell proliferation and/or their survival (17). However, among the T cells recovered from the treated $Rag^{-/-}\gamma c^{-/-}$ mice, a subset of T cells still proliferated in the spleen and in the extralymphoid sites (Fig. 3 B). Moreover, most of the T cells recovered from the extralymphoid organs had divided for multiple times despite CD28/CD154/OX40 blockade treatment (Fig. 3 B). Thus, priming of T cells in vivo by the donor APCs is more resistant to CD28/CD154/OX40 blockade treatment in the absence of NK cells.

Our data suggest that in models where NK cells are impaired or depleted, transplant tolerance to MHC mismatched allografts would be difficult to achieve. To test this possibility in a stringent model, we grafted the full-thickness DBA/2 ($H\text{-}2^d$) skin allografts onto the highly resistant C57BL/6 ($H\text{-}2^b$) recipients (18). The recipient mice were treated with CD28/CD154/OX40 costimulatory blockade with or without NK depletion, and graft survival was determined. As shown in Fig. 4 A, C57BL/6 mice readily rejected the DBA/2 skin allografts with a mean survival time (MST) of 8 d ($n = 7$). Treatment of C57BL/6 mice with transient CD28/CD154/OX40 costimulatory blockade enabled long-term skin allograft survival, and all the DBA/2 skin allografts survived for >100 d ($n = 13$). Interestingly, depletion of NK cells from the recipient mice using a depleting anti-NK1.1 mAb rendered the triple costimulatory blockade protocol completely ineffective at preventing the rejection response, and all NK-depleted and triple blockade–treated mice rejected the DBA/2 skin allografts with a MST of 22 d ($n = 8$). This was in striking contrast to triple blockade–treated mice without NK depletion in which all the DBA/2 skin allografts survived for >100 d.

As shown in Fig. 4 B, transplantation of DBA/2 skin allografts onto CD1d KO mice (NKT deficient) induced prompt skin allograft rejection (MST = 8 d, $n = 5$). Similar to the WT C57BL/6 controls, treatment of the CD1d KO recipients with the triple costimulatory blockade protocol markedly prolonged the skin allograft survival (MST > 50 d, $n = 5$). Interestingly, depletion of NK cells from the triple blockade–treated CD1d KO mice precipitated rapid rejection of the DBA/2 skin allografts (MST = 23 d, $n = 4$). This finding suggests that NK cells, but not NKT cells, are critical to stable skin engraftment in this model.

To ascertain that the requirement for NK cells to enable skin allograft survival is confined to MHC mismatched transplants, we transplanted both DBA/2 ($H\text{-}2^d$) and 129/svJ ($H\text{-}2^b$) skin allografts onto the same C57BL/6 recipients ($H\text{-}2^b$) with or without triple costimulatory blockade and NK depletion. As shown in Fig. 4 C, C57BL/6 mice promptly rejected both the DBA/2 skin grafts (MST = 8 d, $n = 6$) and the multiple minor antigen-mismatched 129/svJ skin grafts (MST = 9 d, $n = 6$). Treatment of recipient mice with CD28/CD154/OX40 costimulatory blockade induced uniform long-term survival of both DBA/2 and 129/svJ skin allografts in the same recipients (MST > 100 d, $n = 6$). Depletion of NK cells in the triple blockade–treated mice precipitated prompt rejection of the DBA/2 skin allografts (MST = 18 d, $n = 6$), but survival of the 129/svJ skin allograft was not affected (MST > 100 d, $n = 6$) (Fig. 4 D). Furthermore, T cells were isolated from C57BL/6 mice that were grafted with DBA/2 skin allografts and treated with the triple costimulatory blockade protocol with or without

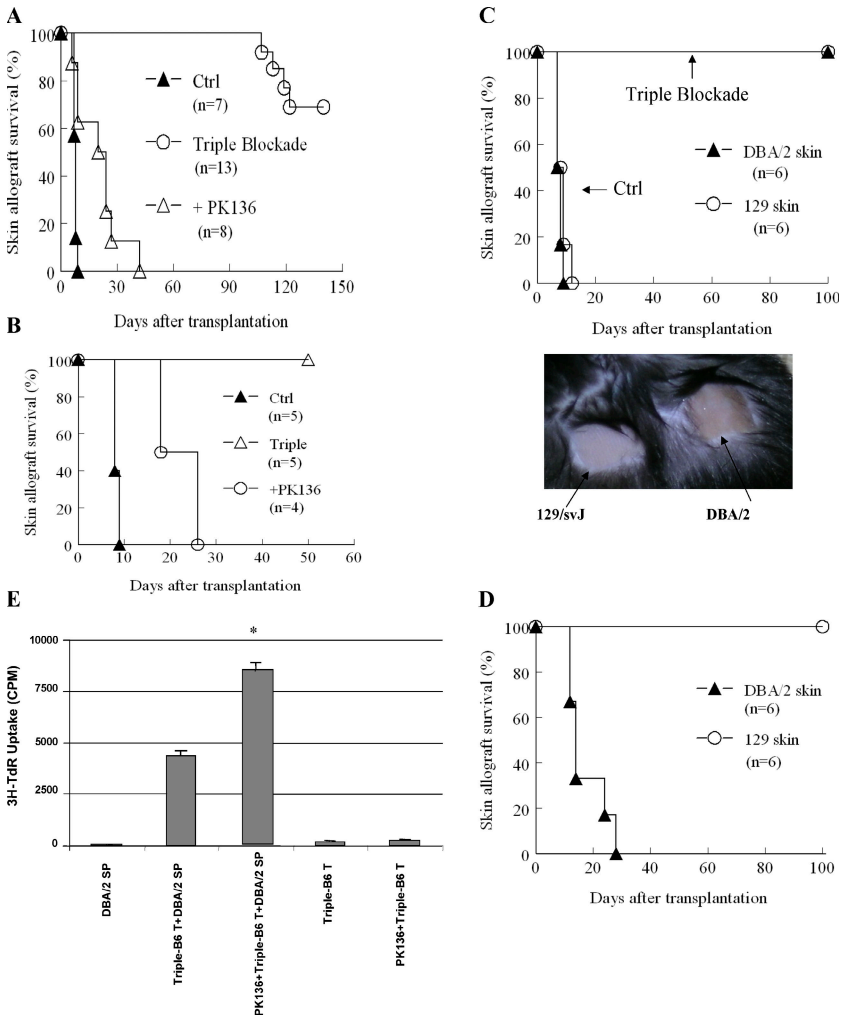

Figure 4. Critical requirement of NK cells in allograft survival. (A) Role of NK cells in CD28/CD154/OX40 costimulatory blockade induced skin allograft survival. C57BL/6 mice were grafted with DBA/2 skin allografts and treated with CTLA4-Ig, anti-CD154, and anti-OX40L. A cohort of recipients was also treated with anti-NK1.1 mAb to deplete NK cells in addition to CD28/CD154/OX40 costimulatory blockade. The skin allograft survival was presented in a Kaplan-Meier plot. *$P < 0.05$. (B) Skin allograft survival in NKT-deficient mice treated with CD28/CD154/OX40 costimulatory blockade protocol with or without NK depletion. (C) Effect of blocking CD28/CD154/OX40 pathways on survival of DBA/2 and 129/svJ skin allografts transplanted onto the same C57BL/6 recipients. DBA/2 and 129/svJ skin grafts were transplanted onto the C57BL/6 recipients. Groups of recipient mice were treated with CD28/CD154/OX40 blockade protocol. Skin allograft survival was presented in a Kaplan-Meier plot. The picture shows healthy skin allografts 100 d after transplantation. (D) Differential requirement of NK cells in survival of DBA/2 and 129/svJ skin allografts induced by CD28/CD154/OX40 costimulatory blockade. C57BL/6 mice were grafted with DBA/2 and 129/svJ skin allografts and treated with CD28/CD154/OX40 blockade protocol. The recipient mice were also treated with a depleting anti-NK1.1 mAb in addition to CD28/CD154/OX40 blockade treatment. Skin allograft survival was presented in a Kaplan-Meier plot. (E) Enhanced T cell priming in vivo in C57BL/6 recipients depleted of NK cells. C57BL/6 mice were grafted with DBA/2 skin allografts and treated with CD28/CD154/OX40 blockade protocol with or without NK depletion. 10 d later, T cells from the host spleen were prepared and stimulated in vitro with mitomycin C–treated donor DBA/2 spleen cells; cell proliferation was determined 3 d later by ^{3}H-TdR uptake assay. Data are presented as mean cpm ± SD of triplicate assays. *$P < 0.05$.

NK depletion. The isolated T cells were rechallenged ex vivo with mitomycin C–treated donor DBA/2 cells, and cell proliferation was determined 3 d later by ^{3}H-TdR uptake assay. As shown in Fig. 4 E, T cells from NK-depleted mice displayed enhanced proliferation compared with those without NK depletion, further confirming that depletion of NK cells resulted in amplified T cell priming in vivo by the donor antigens.

Here we have identified a novel role for NK cells in regulating the adaptive T cell response in transplant models. In contrast to the traditional belief, the cytolytic NK cells are an indispensable cell type for the induction of skin allograft survival. A key role for NK cells in our model appears to control the survival and dissemination of graft-derived donor APCs in transplant recipients, thereby containing the locations and pathways of antigen presentation and the size of alloreactive T cell

clones. Thus, for the highly immunogenic transplants, like the skin where DCs are present in large numbers (15), NK-mediated destruction of certain graft-derived APCs may be one of the critical steps in the acquisition of transplant tolerance.

Our study has several important implications. First, in transplant models, donor-derived APCs can readily accumulate at multiple sites in transplant recipients when NK cells are absent or depleted. As the identity of T cells accumulating at the extralymphoid organs is often different from that in the lymphoid tissues (19), T cell priming at these sites may be an important mechanism of tolerance resistance. However, it remains unclear whether the cytolytic activity of NK cells against donor-derived APCs is mediated by all NK cells or is confined to a specific NK subset. Equally important is the issue as to whether all kinds of donor APCs are sensitive to NK-mediated killing or different cell types are distinct. Second, despite their potent cytolytic activities, NK cells by themselves do not cause damage to the skin allografts. It is well known that NK cells express both stimulatory and inhibitory cell surface receptors (2), and the balanced acts of such positive and negative signals dictate the cytolytic function of NK cells (2). In this regard, our model may provide a valuable tool to further examine whether parenchymal tissues and hematopoietic cells differentially express novel stimulatory or inhibitory ligands for the NK receptors. Finally, our new findings suggest that in solid organ transplantation, therapies that interfere with NK cell function or induce NK tolerance may hinder the induction of tolerance by facilitating the survival and dissemination of donor APCs. Thus, strategies to selectively modulate the cytolytic activities of NK cells may be important in the induction of allograft tolerance, especially to highly immunogenic transplants.

MATERIALS AND METHODS

Animals. DBA/2 (H-2^d), C57BL/6 (H-2^b), Rag1$^{-/-}$ (H-2^b), and 129/SvJ (H-2^b) mice were purchased from The Jackson Laboratory. Rag2$^{-/-}\gamma c^{-/-}$ double mutant mice (H-2^b) were obtained from the Taconic Farm (Germantown, New York). CD1d KO mice on the B6 background (H-2^b) were provided by M. Exley (Beth Israel Deaconess Medical Center, Boston, MA). Animal use and care conformed to the guidelines established by the Animal Care Committee at Harvard Medical School in Boston, MA.

Reagents. The following anti–mouse mAbs were purchased from BD Biosciences: PE anti–mouse CD3 (clone 17A2), cychrome–anti-CD4 (clone GK1.5), cychrome–anti-CD8α (clone 53–6.7), PE–anti–H-2D^d (clone 34–2-12), PE–anti-NK1.1 (clone PK136), and isotype control antibodies. The anti–mouse IFN-γ capture antibody (clone R4-6A2), biotin anti–IFN-γ detection antibody (clone XMG1.2), and streptavidin-conjugated horseradish peroxidase for ELISPOT assays were also obtained from BD Biosciences.

A cell line producing human CTLA–4Ig fusion protein was purchased from the American Type Culture Collection, and the fusion protein was produced by BioExpress. Anti-CD154 mAb (clone MR1), anti-OX40 ligand (OX40L) mAb (clone RM134L), and anti-NK1.1 mAb (clone PK136) used for in vivo studies were manufactured from hybridoma lines by BioExpress and used as previously reported (17, 20).

CD11c$^+$ DC preparation and adoptive transfer. DCs from donor DBA/2 mice were prepared as previously described (21). In brief, CMS-5 cells transfected with the mouse Flt3-ligand gene were injected subcutaneously into DBA/2 mice (40×10^6 cells per mouse). This protocol consistently induces a large number of CD11c$^+$ DCs in the host spleen (21). 10 d later, the mice were killed and total splenic cells were prepared. The spleen cells were then labeled with anti-CD11c–conjugated MicroBeads (Miltenyi Biotec), and CD11c$^+$ DCs were positively isolated using the magnetic-assisted cell sorting (Miltenyi Biotec) according to manufacturer's instructions. The purity of DCs isolated using this method is consistently >90%. The highly purified DCs were adoptively transferred into Rag$^{-/-}$ and Rag$^{-/-}\gamma c^{-/-}$ mice via the tail vein, and $5–6 \times 10^6$ DCs were injected into each mouse for analyses.

T cell labeling with CFSE and adoptive transfer. C57BL/6 mice were killed, and single cell suspension was prepared from the spleen and peripheral lymph nodes. T cells were isolated from such cell preparation using the T cell enrichment columns (R&D Systems) according to the manufacturer's instructions. The purity of T cells isolated using this method is >90% as confirmed by FACS. The purified T cells were then labeled with CFSE (Molecular Probes) as previously reported (22). The CFSE-labeled T cells were washed twice in HBSS before i.v. injection into Rag$^{-/-}$ and Rag$^{-/-}\gamma c^{-/-}$ mice. For the in vivo assays, at least 20×10^6 T cells were injected into each mouse via the tail vein. In some experiments, the Rag$^{-/-}$ and Rag$^{-/-}\gamma c^{-/-}$ mice were injected with allogeneic DCs prepared from DBA/2 mice 2 wk before reconstitution with CFSE-labeled syngeneic T cells.

In vivo CFSE assay. 3 d after injection of host mice with CFSE-labeled T cells, the host mice were killed, and spleen, liver, and lungs were harvested. Spleen cells were prepared as previously reported (23). For isolation of lymphoid cells from the liver and lungs, the organs were first perfused with 0.2% collagenase type IV (Worthington Biochemical Corporation) and then digested at 37°C for 30 min. The digested tissues were disrupted by vigorous vortex, and the lymphoid cells were further isolated by Ficoll gradient centrifugation. The isolated lymphoid cells were resuspended in PBS containing 0.5% BSA and briefly stained with cychrome–anti–mouse CD3 on ice for 15 min. After the staining, cells were washed, fixed in 1% formaldehyde, and analyzed by FACS.

Flow cytometry. All samples were analyzed using a FACSort equipped with CellQuest software (BD Biosciences) (23). Cells were electronically gated based on FCS and SSC parameters to exclude cell debris and dead cells. The phenotype and proliferation of gated cells were analyzed in details. For analysis of in vivo CFSE dilution assays, additional gate was set onto the CD3$^+$ fraction, and the CFSE profiles of CD3$^+$ T cells were presented in histograms with the y axis being relative cell numbers. For phenotypic analysis of gated cells, specific cell staining was presented in histograms or dot plots, and positive staining was calculated as the percentage of total cells gated.

ELISPOT assay. ELISPOT assay was performed to quantitate IFN-γ production by activated T cells as we previously reported (20). In brief, ImmunoSpot plates were coated with 4 μg/ml rat anti–mouse IFN-γ capture mAb (clone R4-6A2) at 4°C overnight. T cells were isolated from the host mice using MACS-assisted cell sorting (Miltenyi Biotec) and then placed in each well (2×10^5 cells/well) in the presence or absence of mitomycin C–treated allogeneic DBA/2 stimulators (8×10^5 cells/well). The plates were cultured in complete RPMI medium (10% FCS, 1% penicillin/streptomycin/L-glutamine) at 37°C for 24 h. Cells were discarded from the plates, followed by washing in PBS containing 0.05% Tween-20. A biotinylated rat anti–mouse IFN-γ detection mAb (clone XMG1.2) (0.5 μg/ml) was added in each well, followed by incubation at 4°C for overnight. The IFN-γ spots were developed using BD AEC substrate reagent set. The spots were then quantitated using a computer-assisted ELISPOT image analyzer (T Spot Image Analyzer; Cellular Technology Ltd.).

Skin transplantation and treatment protocols. Full thickness tail skin grafts from donor mice were transplanted onto the thoracic wall of recipient mice as we reported before (17). Graft survival was assessed by daily

visual inspection, and rejection was defined as the complete loss of viable tissue grafts.

Treatment of recipient mice with the triple costimulatory blockade protocol consisted of CTLA-4Ig (0.5 mg, i.p. on days 1 and 3), anti-CD154 (0.5 mg, i.p. on days 0, 1, 3, and 6), and anti-OX40L mAb (0.5 mg, i.p. on days 0, 2, 4, and 8). Day 0 is defined as the time of skin transplantation.

NK depletion. Depletion of NK cells in vivo in transplant recipient mice was induced by i.p. injection of a depleting anti-NK1.1 mAb (clone PK136). The depleting mAb was given at 0.5 mg i.p. on days –2, 0, and 2 during skin grafting. This protocol has proven potency in depleting all the $NK1.1^+$ cells in the periphery (9).

^{3}H-TdR incorporation. C57BL/6 mice grafted with DBA/2 skin allograft were treated with CD28/CD154/OX40 costimulatory blockade protocol with or without NK cell depletion. 10 d later, the recipient mice were killed and spleen cells were prepared in complete RPMI 1640 medium supplemented with 10% FCS and 1% penicillin/streptomycin. Cells were then plated in 96-well tissue culture plates (2×10^5/well) and stimulated with mitomycin C–treated donor DBA/2 spleen cells (4×10^5/well) in a final volume of 200 μl/well. Cells were cultured at 37°C for 3 d, and for the last 16 h of culture, cells were pulsed with 1 μCi ^{3}H-TdR/well (BD Biosciences), and ^{3}H-TdR uptake was determined by scintillation counting (Beckman Instrument). Results are plotted as mean cpm ± SD of triplicate assays.

Statistics. Difference in skin allograft survival was analyzed by log-rank test. Other data were compared using Student's *t* tests. $P < 0.05$ was defined as significant.

We thank Dr. H. Yagita for his permission to use the anti-CD40L mAb.

This study was supported by the National Institutes of Health (R01 AI057409) and the Juvenile Diabetic Research Foundation International (grant no. 1-2005-129).

The authors have no conflicting financial interests.

Submitted: 17 March 2006
Accepted: 29 June 2006

REFERENCES

1. Yokoyama, W.M., S.H. Kim, and A.R. French. 2004. The dynamic life of natural killer cells. *Annu. Rev. Immunol.* 22:405–429.
2. Lanier, L.L. 2005. NK cell recognition. *Annu. Rev. Immunol.* 23: 225–274.
3. Kumar, V., and M.E. McNerney. 2005. A new self: MHC-class I-independent natural killer cell self-tolerance. *Nat. Rev. Immunol.* 5:363–374.
4. Johansson, S., M. Johansson, E. Rosmaraki, G. Vahlne, R. Mehr, M. Salmon-Divon, F. Lemonnier, K. Karre, and P. Hoglund. 2005. Natural killer cell education in mice with single or multiple major histocompatibility complex class I molecules. *J. Exp. Med.* 201:1145–1155.
5. Ruggeri, L., A. Mancusi, M. Capanni, M. Martelli, and A. Velardi. 2005. Exploitation of allorective NK cells in adoptive immunotherapy of cancer. *Curr. Opin. Immunol.* 17:211–217.
6. Kean, L.S., K. Hamby, B. Koehn, E. Lee, S. Coley, L. Stempora, A.B. Adams, E. Heiss, T.C. Pearson, and C.P. Larsen. 2006. NK cells mediate costimulation blockade resistant rejection of allogeneic stem cells during nonmyeloablative transplantation. *Am. J. Transplant.* 6:292–304.
7. McNerney, M.E., K.M. Lee, P. Zhou, L. Molinero, M. Mashayekhi, D. Guzior, H. Sattar, S. Kuppireddi, C.R. Wang, V. Kumar, and M.L. Alegre. 2006. Role of natural killer cell subsets in cardiac allograft rejection. *Am. J. Transplant.* 6:505–513.
8. Uehara, S., C.M. Chase, W.H. Kitchens, H.S. Rose, R.B. Colvin, P.S. Russell, and J.C. Madsen. 2005. NK Cells Can Trigger Allograft Vasculopathy: The Role of Hybrid Resistance in Solid Organ Allografts. *J. Immunol.* 175:3424–3430.
9. Beilke, J.N., N.R. Kuhl, L.V. Kaer, and R.G. Gill. 2005. NK cells promote islet allograft tolerance via a perforin-dependent mechanism. *Nat. Med.* 11:1059–1065.
10. Auchincloss, H., Jr., and H. Sultan. 1996. Antigen processing and presentation in transplantation. *Curr. Opin. Immunol.* 8:681–687.
11. Li, X.C., T.B. Strom, L.A. Turka, and A.D. Wells. 2001. T cell death and transplantation tolerance. *Immunity.* 14:407–416.
12. Zhou, P., K.W. Hwang, D. Palucki, O. Kim, K.A. Newell, Y.X. Fu, and M.L. Alegre. 2003. Secondary lymphoid organs are important but not absolutely required for allograft responses. *Am. J. Transplant.* 3:259–266.
13. Lakkis, F.G., A. Arakelov, B. Konieczny, and Y. Inoue. 2000. Immunologic 'ignorance' of vascularized organ transplants in the absence of secondary lymphoid tissue. *Nat. Med.* 6:686–688.
14. Cao, X., E.W. Shores, J. Hu-Li, M.R. Anver, B.L. Kelsall, S.M. Russell, J. Drago, M. Noguchi, A. Grinberg, and E.T. Bloom. 1995. Defective lymphoid development in mice lacking expression of the common cytokine receptor gamma chain. *Immunity.* 2:223–238.
15. Kissenpfennig, A., S. Henri, B. Dubois, C. Laplace-Builhe, P. Perrin, N. Romani, C.H. Tripp, P. Douillard, L. Leserman, D. Kaiserlian, et al. 2005. Dynamics and function of Langerhans cells in vivo: Dermal dendritic cells colonize lymph node areas distinct from slower migrating Langerhans cells. *Immunity.* 22:643–654.
16. Goldrath, A.W., L.Y. Bogatzki, and M.J. Bevan. 2000. Naive T Cells Transiently Acquire a Memory-like Phenotype during Homeostasis-driven Proliferation. *J. Exp. Med.* 192:557–564.
17. Demirci, G., F. Amanullah, R. Kewalaramani, H. Yagita, T.B. Strom, M.H. Sayegh, and X.C. Li. 2004. Critical role of OX40 in CD28 and CD154 independent rejection. *J. Immunol.* 172:1691–1698.
18. Williams, M.A., J. Trambley, J. Ha, A.B. Adams, M.M. Durham, P. Rees, S.R. Cowan, T.C. Pearson, and C.P. Larsen. 2000. Genetic Characterization of Strain Differences in the Ability to Mediate CD40/CD28-Independent Rejection of Skin Allografts. *J. Immunol.* 165:6849–6857.
19. Masopust, D., V. Vezys, A. Marzo, and L. Lefrancois. 2001. Preferential localization of effector memory cells in nonlymphoid tissue. *Science.* 291:2413–2417.
20. Vu, M.D., M.R. Clarkson, H. Yagita, L.A. Turka, M.H. Sayegh, and X.C. Li. 2006. Critical, but Conditional, Role of OX40 in Memory T Cell-Mediated Rejection. *J. Immunol.* 176:1394–1401.
21. Meyers, J.H., S. Chakravarti, D. Schlesinger, Z. Illes, H. Waldner, S.E. Umetsu, J. Kenny, X.X. Zheng, D.T. Umetsu, R.H. DeKruyff, et al. 2005. TIM-4 is the ligand for TIM-1 and TIM-1-TIM-4 interaction regulates T cell population expansion. *Nat. Immunol.* 6:455–464.
22. Wells, A.D., H. Gudmundsdottir, and L.A. Turka. 1997. Following the fate of individual T cells throughout activation and clonal expansion. *J. Clin. Invest.* 100:3173–3183.
23. Vu, M.D., F. Amanullah, Y. Li, G. Demirci, M.H. Sayegh, and X.C. Li. 2004. Different costimulatory and growth factor requirements for CD4+ and CD8+ T cell mediated rejection. *J. Immunol.* 173:214–221.